Review Article
cnj.araku.ac.ir

☑ Cite This: Colloid Nanosci. J. 3(3) (2025) 707-726 DOI: 10.61882/CNJ.3.3.707

Ultrasonic-assisted synthesis of nanoporous HZSM-5 ($Na_{14.88}Al_{15.26}Si_{32.74}O_{96}$) and lanthanum and vanadium ion exchange HZSM-5 for biodiesel production via transesterification of canola oil

Maryam Haghighi*, Sedigheh Salehi Shahrbabaky

Department of Physical Chemistry and Nanochemistry, Faculty of Chemistry, Alzahra University, Tehran, Iran

ARTICLE INFO

Article History:
Received 2025-12-10
Revised 2026-01-06
Accepted 2026-01-07
Published 2026-01-09

Corresponding Authors:
Maryam Haghighi
Email:
m.haghighi@alzahra.ac.ir

ABSTRACT

In this study, nanocrystalline HZSM-5 ($Na_{14.88}Al_{15.26}Si_{32.74}O_{96}$) was successfully synthesized in high yield within 24 h using a seed-assisted, template-free, and ultrasonic-assisted method. The optimal pH for HZSM-5 synthesis was determined to be 12.5. Furthermore, the synthesized HZSM-5 zeolite (Z2S4) was modified with lanthanum(III) nitrate and vanadium(III) chloride to produce the xLa/Z2S4 and xV-yLa/Z2S4 catalysts through La^{3+} and V^{3+} ion exchange with H^{+}. The xLa/Z2S4 was applied for transesterification of canola oil for biodiesel production. The molecular weight and consequently the fatty acid compositions of the canola oil were determined using GC-mass analysis. The effect of different parameters on conversion% of canola oil, including La content, zeolite calcination temperature, transesterification temperature, catalyst wt%, methanol-to-oil mass ratio, and reaction time were studied. The optimal La content was determined to be 5 wt%, and the corresponding catalyst was designated as 5La/Z2S4.

The 5La/ZSM-5 exhibited considerable catalytic activity in transesterification of canola oil compared with the parent HZSM-5 zeolite. The catalytic activity of 5La/Z2S4 can be improved by increasing its acidity and specific surface area. The transesterification process achieved a conversion% of 100% using 5La/Z2S4 catalyst calcined at 550 ℃, under the following conditions: methanol-to-oil mass ratio of 15:1, reaction temperature of 85 ℃, reaction time of 7 h, and catalyst loading percent of 20 *wt* %. The results show, that addition of vanadium to 5La/Z2S4 to form a bi-metallic catalyst 0.8V-5La/Z2S4, promoted the catalytic activity in biodiesel production compared to the other synthesized catalysts including 5Ni/Z2S4, 5Cu/Z2S4, 5Co/Z2S4, and 5Cr/Z2S4.

KEYWORDS: *Canola oil; ZSM-5; Biodiesel; Transesterification; Lanthanum*

1. Introduction

Concerns about environmental pollution from CO_2 emissions and sulfur oxides, along with the depletion of fossil fuel sources, have motivated widespread research into sustainable energy sources [1]. The clean and renewable energies restrict the ever-increasing global warming and climate change. Biodiesel, composed of fatty acid methyl esters, is a renewable, carbon-neutral fuel source [2]. Biodiesel combustion generally decreases the levels of sulfur oxides, SO_2 and SO_3 [3]. Furthermore, biodiesel is biodegradable, non-toxic, and a renewable energy source. Therefore, this green, sustainable fuel is considered a viable alternative for solving the energy crisis and environmental pollution problems owing to its superior properties [4, 5]. Natural oils can be used to produce alkyl esters for use in conventional diesel engines (with appropriate cetane number, calorific value, cloud point, pour point, and higher oil solubility), thereby making them suitable as fuels [6, 7]. Previous investigations have demonstrated that biodiesel can be utilized in unmodified diesel engines since it has similar chemical properties to petroleum light oil.

In this endeavor, many efforts have been made to use biodiesel in diesel engines to minimizing environmental issues [8, 9]. Economic studies show that biodiesel may not compete with fossil fuels due to its higher production costs. However, the fabrication cost can be reduced by using less expensive alternative raw materials, such as unrefined oils, non-edible oils, or waste oils [10]. Commonly, the non-edible oils have been taken into consideration as the main source of biodiesel production [11]. Biodiesel can be produced from two pathways: esterification of free fatty acids (FFAs) or transesterification of oils and fats with simple alcohols. Transesterification of triglycerides or esterification of free fatty acids by methanol or ethanol produces an alkyl ester, called biodiesel. Animal fats or vegetable oils with high free fatty acid content were considered the main feedstocks for biodiesel production. Among them, oil crops have received much more attention due to the high oil content of their seeds [12]. Biodiesel has been produced from conventional feedstocks such as soybean, sunflower, palm, and rapeseed [13]. One of the oil-rich seeds is rapeseed, a member of the brassica family [14]. Canola oil is obtained from rapeseed that contains a variety of triglycerides, which can be used to produce biodiesel [15]. Canola cultivars have been harvested in many European countries as a primary source for biodiesel production [16]. The production rate of rapeseed oil in Iran has been increasing in recent years, but its use for industrial applications, such as biodiesel production, is very limited [17]. Canola has the highest productivity per hectare in Iran [18], so canola oil was selected for catalytic biodiesel production.

The esterification reaction is normally performed in the presence of acidic homogeneous catalysts, such as sulfuric acid, sulfonic acid, and phosphoric acid [19, 20]. Homogeneous acid catalysts, especially inorganic acids, can cause corrosion problems with diesel engines or automobile exhaust systems, which should be neutralized at the end of fuel processing. Despite the homogeneous acidic catalysts, heterogeneous base catalysts can be applied in biodiesel production without a further purification process due to their non-corrosive properties [21-24]. Unfortunately, the saponification reaction of FFAs is often harmful to base catalysts, which can deactivate their active sites. Esterification or transesterification reactions can proceed using heterogeneous acidic catalysts without saponification. In general, much research focuses on the synthesis of heterogeneous catalysts due to their easier separation from the reaction environment, reusability, and reduced corrosion. Although biodiesel production may encounter other issues, such as catalyst regeneration and environmental pollution [25, 26].

The main goal of this study is to produce biodiesel from canola oil using methanol with different catalysts. Among the developed catalysts, zeolites have received much more attention due to their promising properties, including reusability, strong acidic sites, a high specific surface area, tunable pore size, high thermal and mechanical stability, a cost-effective synthesis method, and fast, facile separation of the reaction mixture [27-33]. In this study, ZSM-5 was used as a catalyst support via a seed-assisted method. The goal of this study is to design high-porosity ZSM-5 using highly pure, cost-effective N, N-diethylaniline. The authors also focused on producing a La/ZSM-5 catalyst that meets the required specifications for biodiesel production. In addition, zeolites were modified with other transition metals, including Ni, Cu, Co, Cr, and V, in this study.

2. Experimental methods

2. 1. Chemicals

Sodium hydroxide, silicon dioxide, and sodium aluminate were used for zeolite synthesis (Merck). Chromium(III) nitrate, lanthanum(III) nitrate, vanadium(III) chloride, nickel(II) acetate tetrahydrate, cobalt(II) nitrate hexahydrate, copper(II) nitrate, polyethylene glycol (surfactant), hydrochloric acid (solvent), n-hexane (solvent) were supplied from Merck. In addition, absolute ethanol and methanol were supplied from Ghatran Shimi Co. N,N-diethylaniline (Merck Co.) was applied as a structure-directing agent for ZSM-5 synthesis. Canola oil was purchased from Iranian company Famila and applied for transesterification reaction. All chemicals were used in this study as received without further purification.

2. 2. Instruments

In this study, X-ray diffraction (XRD) patterns were reported by a Philips X-ray diffractometer (Cu Kα1 radiation, cobalt anode, the wavelength of 1.7889 Å, 40 kV, 40 mA). FT-IR spectra were recorded on Bruker model Tensor 27 Spectrophotometer. The structural characteristics of formed catalysts were determined using a scanning electron microscope SEM instrument, model EM 3200, kyky, and further information was collected by a Field Emission Scanning Electron Microscope (FESEM) model TESCAN. The elemental analysis of the catalysts was obtained by EDS (model: TESCAN-Sirius SD) apparatus. The unknown samples and products of the transesterification reaction were identified by a gas chromatography-mass spectrometry (GC-MS) analyzer (Model: Agilent 6890N Network GC system -5973N Mass selective detector). An ultrasonic bath (model Transsonic TI-H-5, Elma, Singen, Germany) was employed for homogenizing the mixtures, with power of 70 W at temperature of 70℃. In addition, the concentration and content of various components in the products were measured using a gas chromatography (GC) instrument (Agilent, 6890 series). By BET instrument (Micromeritics TriStar) the specific surface areas of different samples can be measured, including the pore size distribution and specific surface area using nitrogen adsorption isotherms.

2. 3. Synthesis of S3 and S4 seeds

The seed-assisted method is a two-step procedure for zeolite synthesis aimed at reducing the consumption of structure-directing agents (SDAs) and air pollution from burning organic compounds. This method is also considered a facile, low-cost synthesis method compared to conventional methods [34, 35]. The silica gel was prepared by dissolving 1.53 g of SiO_2 in 6 mL of double-distilled water under stirring. In continuation, 0.082 g of sodium aluminate and 0.0065 g of NaOH were dissolved in distilled water (4 ml), followed by the addition of 2.92 g of N, N-diethylaniline as SDA and 5 ml of absolute ethanol. The mixture was stirred continuously for 20 min at room temperature to achieve a transparent solution. In continuation, the mixture was added to the prepared silica gel and stirred with a magnetic mixer (1400 rpm) for 24 h; the solution was then subjected to ultrasonication for 75 min to produce a homogeneous gel. Afterward, the solution was transferred to a stainless-steel autoclave with a Teflon liner and hydrothermally treated at 165 ℃ for 120 h. The particles were separated by centrifugation, washed once with absolute ethanol, and then three times with distilled water. The obtained particles were dried overnight at 120℃. The sample was calcined at 550℃ for 6 h, and the white precipitate produced is called S4. To assess the effect of ultrasonic iiradiation on seed quality, the seeds were synthesized under identical conditions without ultrasonic irradiation, and the obtained seed was nominated S3.

2. 4. Seed-assisted synthesis of ZSM-5 at different pH values (ZS4, Z1S4, Z2S4, and Z3S4) and control sample ZS3

ZSM-5 was synthesized using a seed-assisted method. In this template-free synthesis, a specific amount of seed was added to the initial sodium aluminosilicate gel. The gel composition was identical to that used for seed preparation, except that no organic templates were used. In a beaker, 0.703 g of sodium aluminate was dissolved in 28 ml of distilled water, followed by the addition of 2.52 g of NaOH to adjust the pH of the produced sodium aluminate gel to 11. The mixture was stirred until a clear solution formed. In addition, 5.15 g of SiO_2 was dissolved in 50 ml of distilled water to obtain silica gel. The silica gel was mixed with sodium aluminate solution and stirred vigorously for 150 min to obtain a white mixture (solution 1).

Subsequently, a specific amount of S4 seeds (2.56 g) was added to 9 ml of ethanol to prepare a clear suspension. The seed suspension was

sonicated for 2 h. The obtained suspension was added to the sodium aluminosilicate gel (solution 1) and was stirred for 2 h at room temperature to prepare a homogeneous gel. The suspension was then transferred to a 100 ml autoclave to be treated hydrothermally in a furnace at 165 ℃ for 24 h. In continuation, the nanocrystalline ZSM-5 particles were collected by centrifugation, washed with acidic ethanol (100 ml of ethanol/0.1 ml of HCl 1 M), and subsequently washed several times with distilled water. The collected particles were dried at 130 ℃ in an oven overnight to obtain the ZS4 zeolite. The synthesis was carried out using 2.56 g of S3 seeds (without-ultrasonic irradiation) to produce the ZS3 control sample. In this study, the effects of pH values were examined resulting of various zeolites, as summarized in Table 1.

2. 5. Metal loading on Z2S4 zeolite for the preparation of xM/Z2S4 catalysts (M=La, V, Ni, Cu, Co, and Cr)

Various metals, including La, V, Ni, Cu, Co, and Cr, were immobilized on nano-porous zeolites, and their catalytic efficiencies in the transesterification reaction were comprehensively studied. All catalysts were prepared using the same procedure, with slight variations in metal loading percentages and calcination time during the metal immobilization step. Subsequently, a bimetallic nano-catalyst composed of lanthanum (La) and vanadium (V) was employed to produce biodiesel from canola oil. Evaluation of the catalytic efficiencies revealed that Z2S4 exhibited the highest catalytic activity and the most favorable structural characteristics among the other supports. In this regard, among the synthesized zeolites, Z2S4 was selected as the support for catalyst preparation.

0.0237g of $La(NO_3)_3$ was dissolved in 50 ml of ethylene glycol and was stirred vigorously. In continuation, 0.4 g of NaOH was added to this solution and mixed for 30 min to achieve a white solution. This solution was refluxed at 160 ℃ for 3 h, yielding a brown solution. In the next step, 2 g of prepared Z2S4 was added to this solution and mixed for 24 h at room temperature. The obtained precipitate was separated by centrifugation and washed several times with double-distilled water. The precipitate was dried at 120 ℃ for 14 h and calcined at 550 ℃ for 3 h. The obtained nanocatalyst was designated 0.5La/Z2S4, where 0.5 denotes the La-to-Z2S4 weight ratio. The other catalysts were synthesized through a similar procedure with different metals (Table 2).

2. 6. Catalytic transesterification of canola oil for biodiesel production

Transesterification of triglycerides into fatty acid methyl esters was performed in a jacketed 100 ml batch reactor equipped with a reflux condenser and a magnetic stirrer. Initially, 0.2 g of heterogeneous solid catalyst and 6.075 g of methanol were mixed in a 100 ml reactor equipped with a reflux condenser and a magnetic stirrer (rpm = 700) for 5 min. Afterward, 2 g of canola oil was added to the mixture under vigorous stirring, and the mixture was refluxed for 7 h. The system was heated to the desired temperature, and the mixing rate was maintained at 1000 rpm throughout the reaction. After 7 h of transesterification, the reaction mixture was centrifuged at 3500 rpm for 10 min to separate the catalyst from the solution. Methanol was separated from the mixture by vacuum filtration, after which the solution was poured into a separating funnel and left to stand at ambient temperature overnight, yielding two distinct liquid phases. Two layers formed: biodiesel (the upper layer, comprising biodiesel and the remaining oil) and glycerol (the lower layer). The biodiesel and glycerol layers had different densities, allowing easy separation. The methyl ester content

Table 1. List of zeolites synthesized using S3 and S4 seeds*

Zeolite	Seed type	pH
ZS3**	S3	11
ZS4	S4	14
Z1S4	S4	13.7
Z2S4	S4	12.5
Z3S4	S4	11.4

* 2.56 g of S4 was dissolved in 9 ml of ethanol
**ZS3 is control sample

of the biodiesel phase was determined by gas chromatography. To evaluate catalytic activity, the conversion percentages of canola oil in the transesterification reactions were calculated and compared.

$$Conversion\% = \left(\frac{C_0 - C_e}{C_0}\right) \times 100 \quad (1)$$

In which C_0 and C_e are the initial and remaining concentrations of feed, respectively. According to Eq. 1, the reaction conversion percent was obtained from the peak areas of the GC spectrum. The reaction operating conditions, such as catalyst amount, methanol-to-oil mass ratio, reaction time, and temperature, were optimized to achieve the highest efficiency.

3. Results and discussion

3. 1. FTIR spectra of the samples

The FTIR spectrum of the S4 seed is presented in Fig. 1. The peaks observed at 470 cm^{-1} and 804 cm^{-1} correspond to the bending and symmetric stretching vibrations of T–O–T (T=Al or Si), respectively. The peak appeared at 1100 cm^{-1} is attributed to the asymmetrical stretching vibration of T–O–T [36]. The absorption peaks around 1500 cm^{-1} are assigned to the symmetric and asymmetric stretching vibrations of T–O–T of SiO_4 and AlO_4 tetrahedron (T=Al or Si), as well as to the bending vibrations of Si–O–H. Moreover, the absorption

Table 2. List of synthesized catalysts

Zeolite	Metal type	wt/wt (%)	Calcination temperature (°C)
0.5La/Z2S4	La	0.5% (0.0237g of $La(NO_3)_3$ and 2 g of Z2S4)	550
1La/Z2S4	La	1% (0.0473 g of $La(NO_3)_3$ and 2 g of Z2S4)	550
2La/Z2S4	La	2% (0.0945 g of $La(NO_3)_3$ and 2 g of Z2S4)	550
3La/Z2S4	La	3% (0.142 g of $La(NO_3)_3$ and 2 g of Z2S4)	550
4La/Z2S4	La	4% (0.19 g of $La(NO_3)_3$ and 2 g of Z2S4)	550
5La/Z2S4	La	5% (0.237 g of $La(NO_3)_3$ and 2 g of Z2S4)	300, 400, 550, 700
6La/Z2S4	La	6% (0.284 g of $La(NO_3)_3$ and 2 g of Z2S4)	550
7La/Z2S4	La	7% (0.331 g of $La(NO_3)_3$ and 2 g of Z2S4)	550
5V/Z2S4	V	5% (0.308 g of VCl_3 and 2 g of Z2S4)	550
5Ni/Z2S4	Ni	5% (0.424 g of Ni $(CH_3COO)_2.4H_2O$ and 2 g of Z2S4)	550
5Cu/Z2S4	Cu	5% (0.295 g of $Cu(NO_3)_2.3H_2O$ and 2 g of Z2S4)	550
5Co/Z2S4	Co	5% (1.039) g of $Co(NO_3)_2.6H_2O$ and 2 g of Z2S4)	550
5Cr/Z2S4	Cr	5% (0.4577 g of $Cr(NO_3)_3$ and 2 g of Z2S4)	550
0.8V-5La/Z2S4	V and La	0.8%V and 5%La (0.049g of VCl_3 and 0.237g of $La(NO_3)_3$ and 2 g of Z2S4)	550

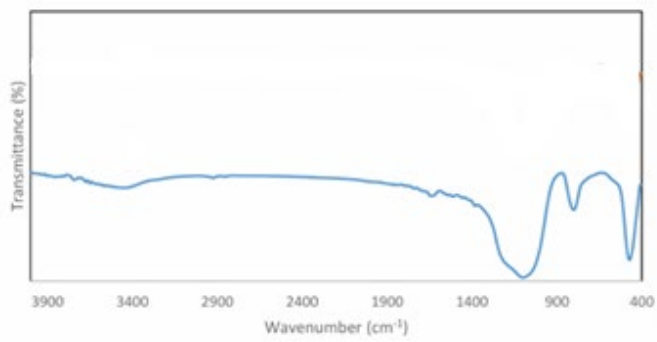

Fig. 1. FTIR spectrum of S4

peaks in the range of 2800–3000 cm^{-1} and the broad peak at 3400–3500 cm^{-1} are attributed to the asymmetric C–H stretching vibration of methylene groups and the O–H stretching of the Si–OH–Al bridge (indicative of Brønsted acid sites), respectively [22, 23].

Subsequently, the FTIR spectra of ZS4, Z1S4, Z2S4, and Z3S4 were obtained and are shown in Fig. 2. The peaks appeared at locations similar to those of the synthesized seeds, with only slight variations. The observed peaks at 1500 cm^{-1} In Fig. 2, it relates to symmetric and asymmetric stretching vibrations of T-O-T in the TO4 tetrahedron (T = Si, Al) and five-membered rings of pentasil in zeolite, and bending vibrations of T-OH (T = Si, Al) in ZSM-5 [37, 38]. The bands at 470 cm^{-1} and 804 cm^{-1}, which represent the five-membered ring pentasil unit of the ZSM-5 structure and indicative of zeolite crystallinity.

In continuation, FTIR spectra of the prepared metal-loaded catalysts (5La/Z2S4, 5V/Z2S4, 5Ni/Z2S4, 5Co/Z2S4, 5Cu/Z2S4, and 5Cr/Z2S4) have been compared with the FTIR spectrum of Z2S4 in Fig. 3. Comparison of the spectra in Figs. 3b–g with that of Z2S4 (Fig. 3a) indicates no significant differences. This confirms that Z2S4 retained its structure after cation substitution. The slight shifts observed in the Z2S4 peaks can be attributed to ion exchange within the zeolite structure. For instance, the peaks at 553 cm^{-1} and 621 cm^{-1} in the Z2S4 spectrum (Fig. 3a), corresponding to the T-O-T inner stretching vibrations, are diminished, weakened, or shifted following metal deposition. The shift in the Si-OH stretching vibration is associated with interactions between Si-OH groups and metal ions. This provides evidence that a substantial number of internal Si–OH groups within the zeolite rings coordinate to the metal ions, forming Si–O–M bonds (M = La, V, Ni, Co, Cu, Cr). Additionally, the intensity of the OH peak in the range of 3500-3800 cm^{-1} has decreased and transferred, indicating a decline in the number of OH bridges in Al-OH-Si, which is due to replacement by M-OH (La-OH) [39-41].

Fig. 4. presents the FTIR spectrum of the 0.8V-5La/Z2S4 bimetallic catalyst, compared with

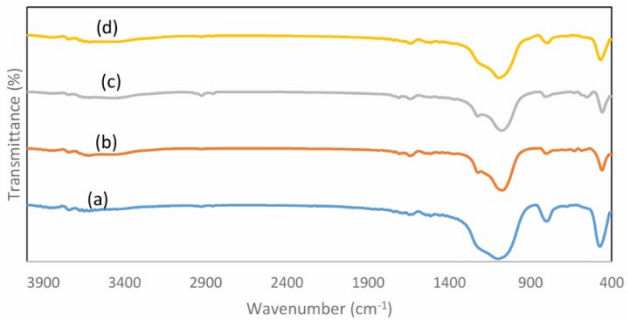

Fig. 2. FTIR spectra of (a) ZS4, (b) Z1S4, (c) Z2S4, and (d) Z3S4

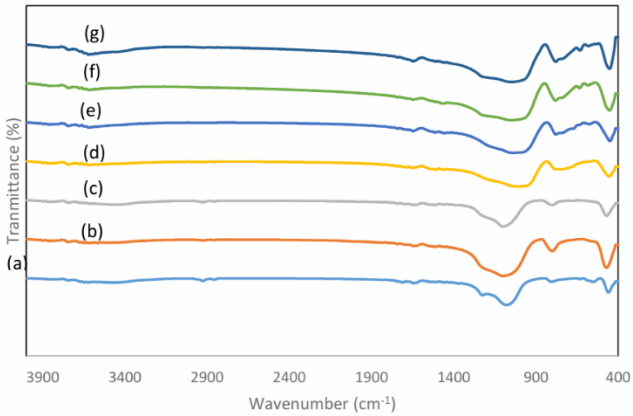

Fig. 3. FTIR spectra of (a) Z2S4, (b) 5La/Z2S4, (c) 5V/Z2S4, (d) 5Ni/Z2S4, (e) 5Co/Z2S4, (f) 5Cu/Z2S4, and (g) 5Cr/Z2S4

that of the parent Z2S4. The slight shift observed in the FTIR spectrum of Z2S4 is attributed to ion exchange within the zeolite framework. A peak at 630 cm^{-1} corresponds to the La-O vibration, while the broad observed peak in the range of 3400-3600 cm^{-1} is assigned to the OH stretching vibration. The substitution of Al by other metal species (M) in the hydroxyl bridge leads to the formation of BrØnsted acid sites. The presence of Lewis acid sites is evidence by the band appearing in the range of 1450-1490 cm^{-1}. The peak observed in the region of 1425-1480 cm^{-1} is assigned to the bending vibration of the O-V-O group [41, 42].

The FTIR spectra of 5La/Z2S4 before and after the transesterification reaction are presented in Figs. 5a and 5b respectively. The FTIR spectra of the catalyst indicate that the zeolite structure was preserved after the reaction, with no significant changes, which can be attributed to the catalyst's high structural stability. The absorption peaks observed in the range of 2800-3000 cm^{-1} relate to the C-H stretching vibrations of a methylene group (Fig. 5b). This feature indicates the presence of oil or organic impurities adsorbed on the catalyst surface, which could not be completely removed even after washing.

3. 2. EDS Analysis

Elemental analysis of the samples was performed using Energy-dispersive X-ray spectroscopy (EDS), as shown in Figs. 6a-d. Various chemical elements, including silicon, aluminum, sodium, carbon, and oxygen, were detected in all samples, all of which are related to the added compounds in the reaction. Additionally, the detected carbon peak can be attributed to impurities in the sodium aluminate used. The high oxygen content is associated with the presence of aluminate and silica in the reactants. The results show that ultrasonic irradiation could lead to higher Si/Al ratio. The average Si/Al mass ratio of S3 seed (without ultrasonic irradiation) is 14 (Fig. S1), however S4 exhibited an average Si/Al mass ratio of 22.3 (Fig. 6a), which is close to the initial reactant ratio and agrees with the value suggested in reference [43]. Consequently, S4 was selected as a suitable seed and was directly used in the synthesis of ZSM-5. The EDS spectrum of the ZS4 zeolite is reported in Fig. 6b. According to

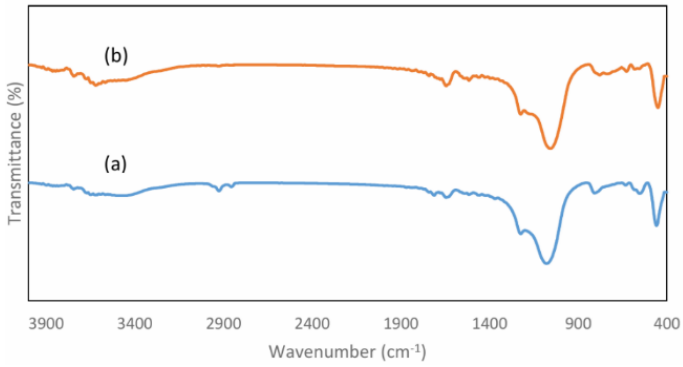

Fig. 4. FTIR spectra of (a) Z2S4, (b) 0.8V-5La/Z2S4

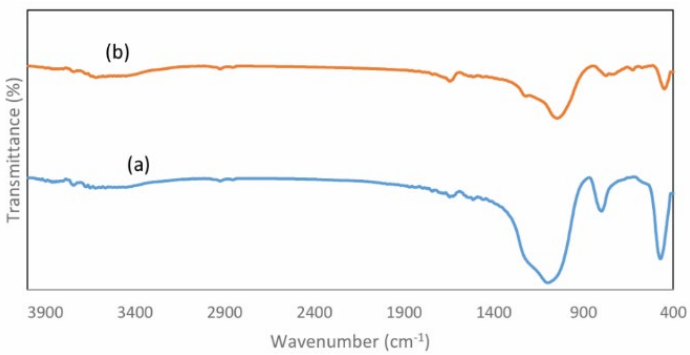

Fig. 5. FTIR spectra of 5La/Z2S4 (a) Before transesterification, and (b) After transesterification

the experimental data, the Si/Al mass ratio of ZS4 was determined to be 7.1. The average Si/Al mass ratio in the Z2S4 sample is approximately 10 (Fig. 6c), which corresponds to the initial Si/Al ratio and is consistent with the value reported in reference [27]. It can be observed that as the pH decreases, the sodium content decreases, while the average Si/Al mass ratio increases. Furthermore, EDS analysis revealed that the average Si/Al mass ratio of Z3S4 was approximately 9 (Fig. 6d), which is close to the initially employed Si/Al ratio. Since the highest Si/Al ratio was obtained at pH=12.5, the Z2S4 zeolite was selected as the optimal zeolite for catalyst synthesis and subsequently metal loading.

Transition metal-loaded zeolites have attracted increasing attention for their high catalytic activity in redox reactions and favorable physicochemical properties. These catalysts have been employed in a variety of organic reactions, such as the oxidation of alkenes, the conversion of olefins to thiols, the separation of nitromethanes, and the production of biofuels [44]. Therefore, different catalysts, including 5V/Z2S4, 5Ni/Z2S4, 5Co/Z2S4, 5Cu/Z2S4, 5Cr/Z2S4, and 5La/Z2S4, were synthesized in this study by loading different transition metals onto the Z2S4 zeolite. Figs. 7a-e show that the metals were well stabilized in the zeolite structure. Notably, the amount of immobilized lanthanum ions is higher than that of nickel, vanadium, copper, and chromium. Subsequently, vanadium and lanthanum were simultaneously stabilized on the surface of Z2S4 in varying amounts to prepare the 0.8V-5La/Z2S4 catalyst. The elemental composition of the catalyst is presented in Fig. 7f. Comparison of the EDS analysis indicates a slight reduction in the amounts of Si, Al, and La, whereas vanadium cations are effectively immobilized within the catalyst structure.

3. 3. SEM analysis

Fig. 8a presents typical S4 seed nanoparticles with sizes ranging from 15 to 60 nm, corresponding to a Si/Al ratio of approximately 22.3. SEM image clearly shows that the particles were synthesized in a uniform, well-ordered manner, with no aggregation or cohesion. Moreover, the morphologies and particle sizes of the samples do not differ significantly. The use of these nanoscale seeds promotes the formation of zeolites with nanoscale dimensions. The average crystal size of the S4 varies between 15 and 60 nm, resulting from a combination of the ultrasonic effect and the hydrothermal synthesis method. The porous and uniform structure of ZS4, consisting of spherical particles, is presented in Fig. 8b.

The morphology of Z2S4 is illustrated in Figs. 9 a-d. It can be observed that the particles are individual, highly uniform, well-ordered, and fully integrated, with no evidence of aggregation or adhesion. Figs. 9c and 9d show the layered

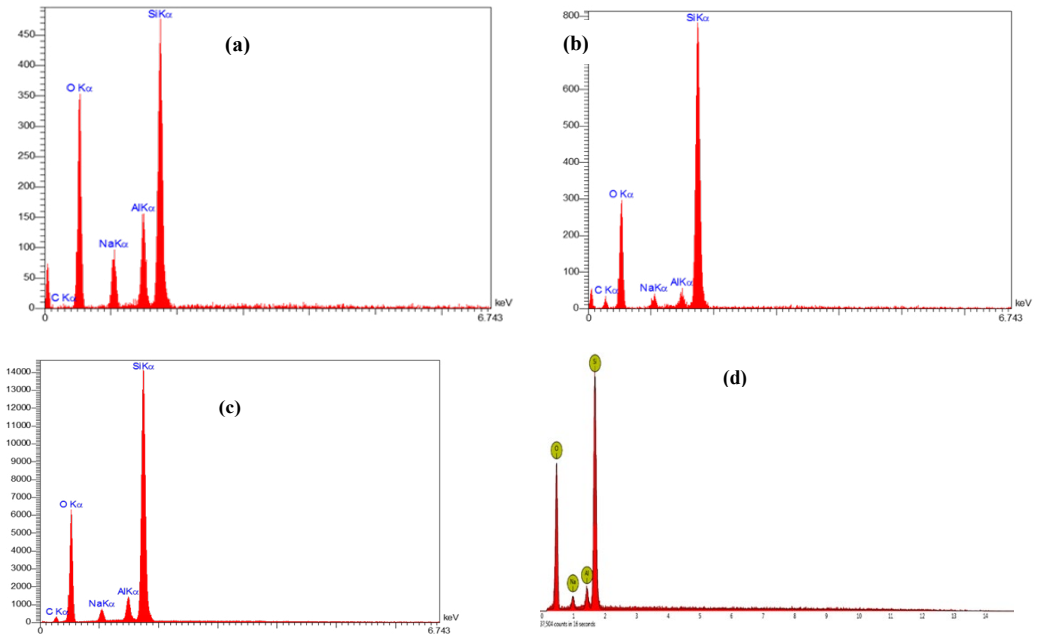

Fig. 6. EDS analysis of synthesized samples (a) S4, (b) ZS4, (c) Z2S4, and (d) Z3S4

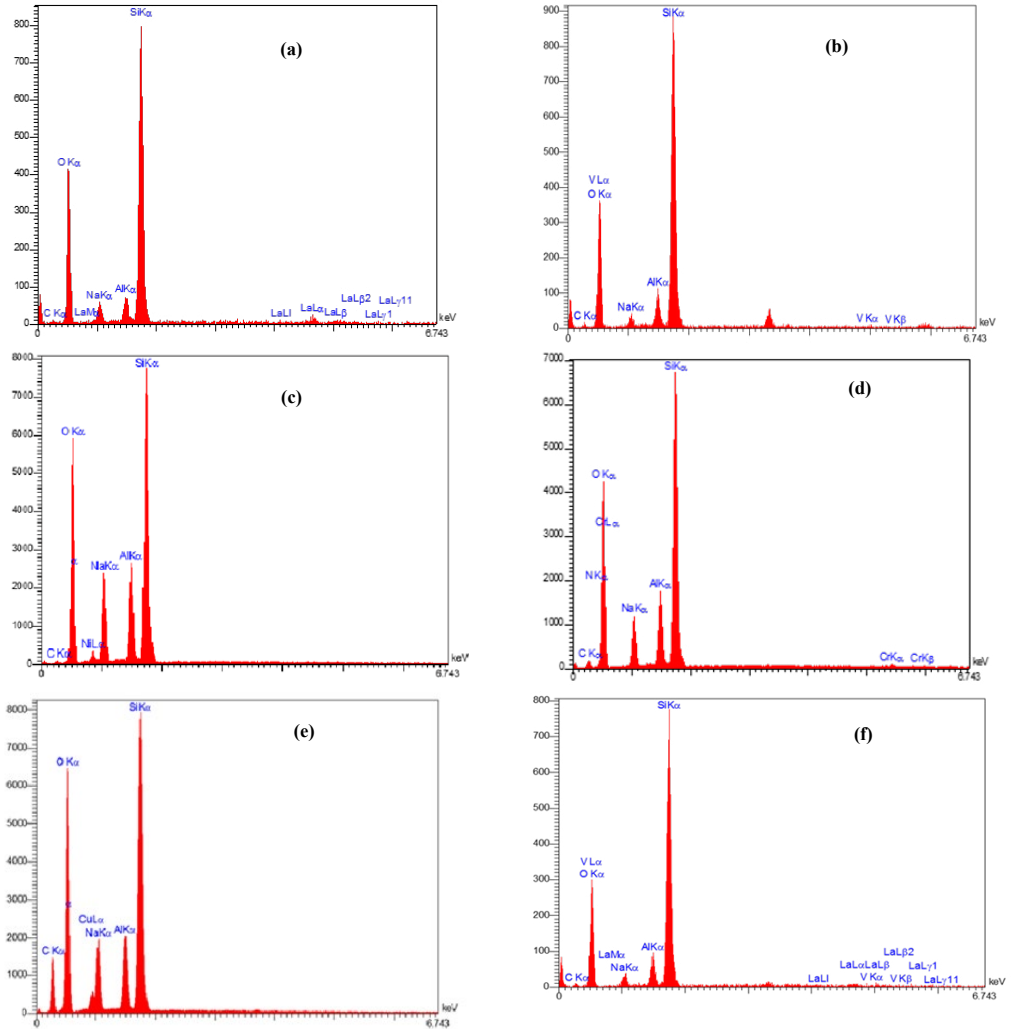

Fig. 7. EDS analysis of metal based-zeolites (a) 5La/Z2S4, (b) 5V/Z2S4, (c) 5Ni/Z2S4, (d) 5Cr/Z2S4, (e) 5Cu/Z2S4, and (f) 0.8V-5La/Z2S4

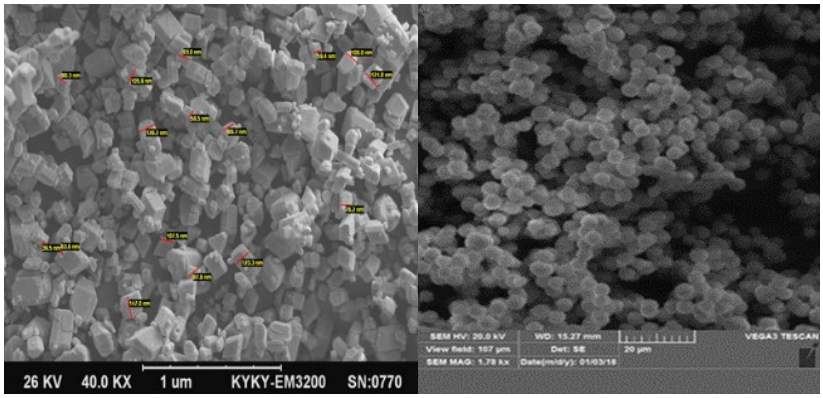

Fig. 8. SEM image of (a) S4 seeds and (b) ZS4

structure of the particles. Each particle is composed of uniform sheets measuring 10-60 nm, which are interconnected to form spherical particles.

The FE-SEM images of the 5La/Z2S4 catalyst (Figs. 10a-d) reveal the layered structure of the particles. Each particle is composed of multiple interconnected sheets that assemble into spherical aggregates. Lanthanum is uniformly immobilized on the Z2S4 zeolite substrate, with particle sizes ranging from 20 to 40 nm (Fig. 10c).

SEM images of the ZS3 control sample (Figs. S2 (a-c)) reveal localized particle aggregation, which may result from non-uniform homogenization in the absence of ultrasonic irradiation. Amorphous particles are also observed in certain. The average particle diameter was found to range between 1 and 2 μm. Due to the low Si/Al ratio of S3 seeds (14) and structural non-uniformity, the ZS3 sample was not employed in the transesterification reaction.

3. 4. XRD results of Z2S4 and 5La/Z2S4 samples

Fig. 11 shows the powder XRD pattern of the prepared Z2S4 zeolite. The sample shows the characteristic diffraction peaks at the angles

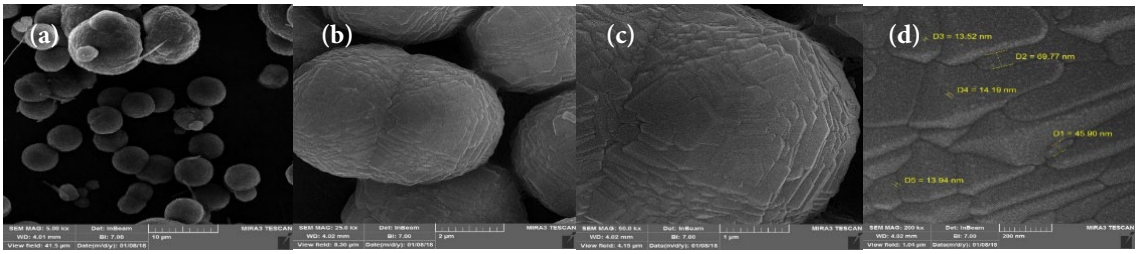

Fig. 9. SEM images of Z2S4 (a) An integrated overview of the zeolite particles, (b) A view of a single particle, (c) Structure of the particle layers, and (d) Size of the layers

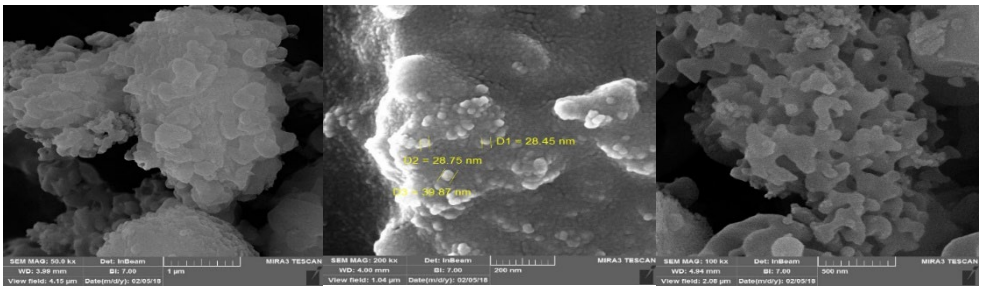

Fig. 10. FE-SEM images of 5La/Z2S4 (a) An overview of the porous zeolite, (b) Aggregation of the particles, and (c) Immobilization of lanthanum on the Z2S4 zeolite

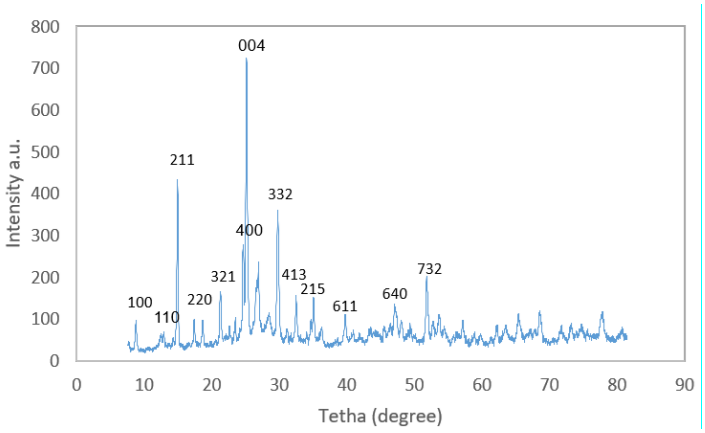

Fig. 11. XRD pattern of Z2S4 sample

2θ of 14.92°, 17.42°, 23.43°, 25.14°, 25.20°, 29.78°, 32.53°, 35.16°, 39.79°, 47.11°, and 51.87°, corresponding to the crystalline planes of 211, 220, 321, 400, 004, 332, 413, 215, 611, 640 and 732 respectively (JCPDS: 6418-89). This structural characteristic identified the ZSM-5 structure corresponds to the $Na_{14.88}Al_{15.26}Si_{32.74}O_{96}$ chemical formula. Also, the observed peaks at the angles of 12.79°, 15.12°, 17.92°, 26.52°, and 28.32° are related to the crystalline planes of 110, 101, 121, 310, and 301, respectively which identified the amorphous hydrated sodium aluminum silicates with the formula $(Na_2O)_{1.31}Al_2O_3(SiO_2)_{2.01}(H_2O)_{1.65}$ with a hexagonal structure.

The mordenite phase, with the chemical formula $Na_2Al_2Si_{13.3}O_{29.6}$ and an orthorhombic system, is also detected in this zeolite, which is not the dominant phase in the zeolite structure. The sharp diffraction peaks in the XRD pattern indicate the high crystallinity of the zeolite particles. A summary of crystallographic data is reported in Table 3.

In continuation, the XRD pattern of the La loaded ZSM-5 (5La/Z2S4) sample was reported to demonstrate the structural stability during metal loading (Fig. 12).

Comparing the XRD diffraction pattern of 5La/Z2S4 with the pattern for Z2S4 shows that after La stabilization, there did no significant change in the zeolite structure; the appeared peaks shifted slightly to larger angles, confirming the placement of the La in the pores of Z2S4. The observed diffraction peaks at the angles 2θ of 22.25°, 27.72°, 30.35°, 31.50°, 33.15°, 34.65°, 35.45°, 40.20°, 44.30°, 50.83°, 51.11°, 54.50°, 56.69°, and 59.76° corresponding to the crystalline planes of 200, 004, 203, 212, 300, 005, 204, 312, 400, 224, 322, 030, 126, and 133 respectively; which are assigned to lanthanum aluminate with the chemical formula $La_{10}Al_4O_{21}$ with an orthorhombic structure (JCPDS: 39-009).

Also, in the 5La/Z2S4 sample, the diffraction peaks are not clear and transparent, which could be because very small amounts of metal oxide particles

Table 3. Crystallographic data of Z2S4

Crystal system	Space group	Space group number	A (Å)	b (Å)	c (Å)	Alpha (°)	Beta (°)	Gamma (°)	Calculated density (g/cm^3)
Tetragonal	141/acd	142	13.6251	13.6251	13.5870	90.000	90.000	90.000	2.11

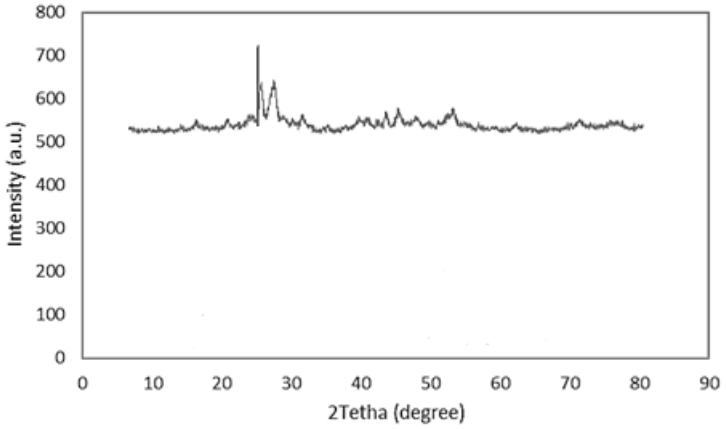

Fig. 12. XRD patterns of 5La/Z2S4

Table 4. BET analysis of Z2S4 structure

Sample	BJH desorption average pore width (nm)	BJH Adsorption average pore width (nm)	Adsorption average pore diameter (nm)	Total pore volume (cm^2/g)	t-Plot External Surface Area (m^2/g)	t-Plot Micropore Area (m^2/g)	BET Surface Area (m^2/g)
ZSM-5	5.6831	3.86	9.5737	0.0203	659.93	190.85	850.79

escape XRD detection. In fact, the La/ZSM-5 sample was prepared by heating at 550°C, and it has been reported that metal oxide can migrate into the pores of the zeolite through calcination process and the migration rate depends on the temperature used [39].

3. 5. Textural properties of Z2S4 as appropriate support for the catalyst

The most common method for measuring the specific surface area of materials is the Brunauer-Emmett-Teller (BET) method. In this technique, the surface area of the zeolites, as well as the cavity diameter and volume, are determined from nitrogen adsorption-desorption isotherms. In this study, the properties of the synthesized and commercial samples were compared. As can be observed in Table 4, the surface area of the synthesized sample is 850.79 m^2/g, which is nearly twice that of the commercial sample [45]. The BET surface area of the commercial ZSM-5 which was reported in reference [45] was reported as 415 m^2/g. The BET surface area of the synthesized sample (Z2S4) was measured as 850 m^2/g which is more than twice than the commercial sample. Also, the surface area of the synthesized sample in the reference [45] (which was dominated ZSM-5-M) was measured as 608 m^2/g which is lower than that of the synthesized Z2S4 sample in this study. An increase in surface area can enhance the catalytic activity of the aforementioned zeolite. Moreover, the synthesized zeolite exhibits a larger pore size than the commercial sample, which may contribute to improved selectivity.

The nitrogen adsorption–desorption isotherms of Z2S4 are shown in Fig. 13 and compared with those of the commercial sample. The results indicate that both types of zeolites exhibit IV-type isotherms, which belong to the fourth category in the IUPAC classification. This result confirms the presence of a mesoporous structure with pore sizes ranging from 2 to 50 nm.

The pore size distribution of Z2S4 is presented in Fig. 14. It can be seen, the overwhelming majority

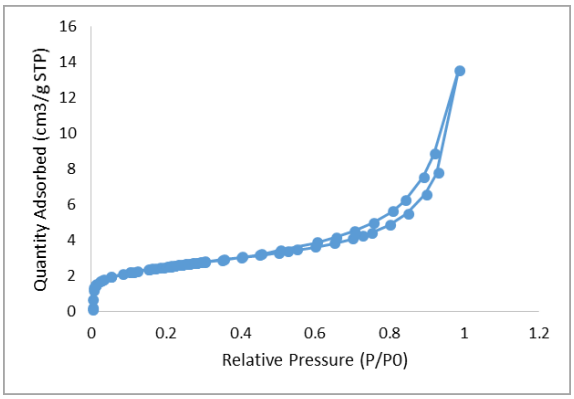

Fig. 13. The nitrogen adsorption-desorption isotherms of the Z2S4 sample

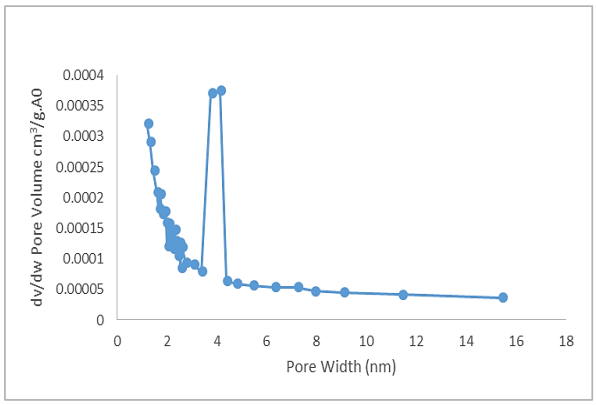

Fig. 14. The pore size distribution of Z2S4

of the pores are distributed within the range of 3-4.5 nm, with an average pore size of 3.8 nm. Additionally, several minor peaks are observed between 2 and 2.7 nm, indicating the presence of smaller pores in this region [45].

3. 6. Identification of canola oil

In this study, canola oil was used as the feedstock for the transesterification process, as it is one of the most widely cultivated plants in the world and is commonly used for animal feed, edible oils, and biodiesel production. Canola oil is a mixture of triglycerides, each consisting of three fatty acids esterified to a glycerol [46]. The catalytic performance of the synthesized catalysts was investigated via the transesterification of canola oil with methanol. Previous research has shown that canola seeds contain approximately 40–48% oil, 38–45% protein, and about 5% moisture. Canola is one of the most important oilseed crops in the world, ranking fourth after soybean, date, and cottonseed [47, 48]. Consequently, canola oil is very low in saturated fatty acids, while the amount of polyunsaturated fatty acids (including oleic acid, linoleic acid, and oleicomega-3 alpha-linolenic acid) is high [49]. The specifications of the canola oil used in this study are summarized in Table 5.

In this investigation, the AOCS Ce 1-62 method was employed to determine the types and compositional percentage of fatty acids. According to this method, triglycerides were first converted into their corresponding methyl esters, and, subsequently, using the GC-mass analyzer, the molecular weight of the methyl esters and thus the types of fatty acids were identified (Fig. 15).

The detected methyl esters, their molecular weights, and retention times were reported in Table 6.

3. 7. Saponification number and molecular weight of canola oil

Saponification number (SN) is defined as the milligrams of potassium hydroxide needed to saponify one gram of oil. The saponification number gives us useful information about the types of fatty acids that are combined with glycerol. The amount of potassium hydroxide needed to saponify

Table 5. Physical properties of the canola oil used in this study

Quantity	Amount
Max fatty acid content (%)	0.1
Max of humidity (%)	0.1
Cinematic viscosity at 40 ℃ (cst)	30.108
Density at 40 ℃ ($g \cdot cm^{-3}$)	0.905
Molecular weight ($g \cdot mol^{-1}$)	894.454

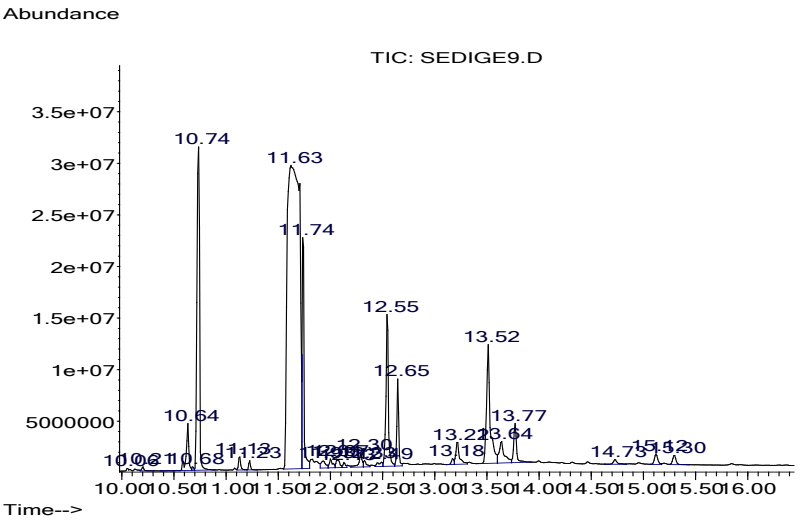

Fig. 15. The GC-mass choromatogram of triglyceride methyl esters of canola oil

various fatty acids is inversely related to their molecular weight. This number actually indicates the length of the fatty acid chain of the sample. In other words, the longer the chain of fatty acids, the lower their SN. By measuring the saponification number, which is, in fact, alkaline hydrolysis of esters, the purity of fats can be determined. To measure the saponification number, a specified amount of canola oil is reacted with a potassium hydroxide solution (potassium hydroxide dissolved in ethanol). After the reaction is complete, the amount of remaining KOH is measured by titration with HCl (0.5 M). The following reactions occur during saponification and titration:

$$R\,COOH + KOH \rightarrow R\,COOK + H_2O \quad (2)$$

$$KOH + HCl \rightarrow KCl + H_2O \quad (3)$$

Afterward, the SN of the oil sample is calculated as follows:

Saponification number =SN

$$= \frac{(B-A)(N_{HCl})\times 56.1}{C} \quad (4)$$

In which B, A, N_{HCl}, and C represent the ml of HCl solution used for the blank run, ml of HCl solution used for the oil sample, normality of HCl solution (0.5), and the weight of the sample in grams, respectively. The molecular weight of KOH is 56.1 g.mol^{-1}. The titration was carried out 5 times, and the average values of A and B were determined to be 7.78 ml and 21.2 ml, respectively. Therefore, the SN of the used canola oil is calculated to be 188.2155. As can be seen in Fig. 16, the soaping reaction proceeds according to the following equation:

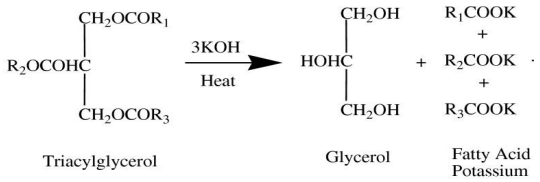

Fig. 16. Schematic illustration of the saponification reaction

Regarding the transesterification reaction, it was found that 3 moles of KOH are required for each mole of triglyceride, then the number of moles of triglyceride per 1 gram of canola oil can be calculated by the following formula:

Number of moles of triglyceride=

$$188.2155\,mg\,of\,KOH \times \frac{1\,mmol\,KOH}{56.1\,mg\,KOH} \times \frac{1\,mol}{1000\,mmol} \times \frac{1\,mol\,triglycerid}{3\,mol\,KOH} = 0.001118\,mol\,triglyceride \quad (5)$$

As a result, 1 gram of oil is equivalent to 1.118 mmol of triglyceride, and the molecular weight of canola oil is 894.454 g.mol^{-1}.

3. 8. Optimization of operating conditions for biodiesel production using xLa/Z2S4

In this research, Z2S4 was selected as the optimal support for metal-decorated catalysts based on the analyses performed. Lanthanum oxide is already known in the literature for biodiesel production as a highly efficient catalyst [39, 50, 51]. Despite the fact that La is an expensive metal, using of very small amounts of La can improve the efficiency of the catalyst superior. Due to this fact La have been used in many studies.

The results show that La stabilization on the zeolite surface creates BrØnsted acidic sites and improves catalytic activity. This is possible in two ways, as explained below. By loading La in the zeolite structure, a lanthanum atom replaces the aluminum atom in the bond of the hydroxyl group of the bridge, and this isomorphic shift creates a new BrØnsted acidic site [39]. Also, during ion exchange between La^{3+} and zeolite, a hydrous metal cation $[La(OH)]^{+2}$ may be formed due to the electrostatic field of the metal cation that results in the new Br∅nsted acidic site as follows:

$$La^{3+} + nH_2O \rightarrow La\left(H_2O\right)_n^{3+} \quad (6)$$

$$La\left(H_2O\right)_n^{3+} \rightarrow La\left(OH\right)_n^{2+} + nH^+ \quad (7)$$

In this investigation, lanthanum-supported ZSM-5 catalysts were synthesized by loading different percentages of $La(NO_3)3.6H_2O$ onto Z2S4 zeolite, and the xLa/Z2S4 catalyst was applied for biodiesel production. Several factors, including the lanthanum content, zeolite calcination temperature, transesterification reaction temperature, catalyst wt%, methanol-to-oil mass ratio, and reaction time influence the efficiency of the transesterification reaction. Accordingly, the effects of these parameters on canola oil conversion were systematically investigated to determine

optimal operating conditions. It should be noted that, in the optimization of each parameter, all other variables were held constant. Multiple experiments were conducted under different conditions, each performed in triplicate. The conversion percentages of canola oil in different conditions were calculated, and the resulting data are presented and compared in Table 7.

Initially, the effect of La content in the catalyst on canola oil conversion was studied. The transesterification of canola oil with methanol was carried out using xLa/Z2S4 catalysts with different weight percent of La (including 0.5, 1, 2, 3, 4, 5, 6, and 7 *wt*%) under operating temperature of 100°C, using of 10 *wt*% of catalyst, and the mass ratio of methanol-to-oil 3:1 (6 g of methanol and 2 g of canola oil) for 7 h (Entries 1-8 of Table7). Increasing the La percentage to 5 *wt*% increases the number of active catalyst sites and the conversion of canola oil. However, with increasing the La loading beyond the optimal value (5 *wt*%), the conversion percentage decreased, which can be attributed to the closure of active sites and thus a reduction in catalyst activity for the transesterification reaction. Therefore, 5La/Z2S4 was selected as the best catalyst, with a conversion of 95.42%.

In continuation, the 5La/Z2S4 catalyst was calcined at different temperatures (300, 400, 550, and 700 °C) to investigate the effect of calcination temperature on the catalytic efficiency of the zeolite. The transesterification reaction of canola oil with methanol was performed using 5La/Z2S4 at a temperature of 100°C with 10 *wt* % of catalyst and a mass ratio of methanol-to-oil of 5:1 for 7 h (Entries 9-12 of Table 7). It was found that increasing the calcination temperature to 550°C increases biodiesel production efficiency, because higher temperatures promote more complete burning of the OSDA, creating conditions for the formation of new cavities and porosity that lead to an increase in surface area. However, increasing the temperature above 550°C reduced the efficiency of biodiesel production, because the catalyst was exposed to agglomeration. According to the experimental results, 550°C was identified as the optimal calcination temperature and selected for subsequent transesterification reactions. The experiments indicated that increasing the reaction temperature increases the reaction rate. Elevated temperatures improve the miscibility of the reactants, thereby promoting more efficient reaction kinetics.

Nevertheless, the maximum operating temperature is limited by the alcohol's boiling point [52]. To investigate the effect of temperature on reaction efficiency, the reaction was conducted using 10 *wt* % of the 5La/ZSM-5 catalyst with a calcination temperature of 550°C, a methanol-to-oil mass ratio of 5:1, at temperatures of 25, 40, 55, 70, 85, 100, and 115°C for 7 h (Entries 13-19 of Table 7). The highest conversion, 100%, was achieved at a reflux temperature of 100°C. At temperatures above 100 °C, the conversion percentage of canola oil decreased. This decline can be attributed to the fact that, at elevated temperatures, adverse reactions—such as the hydrolysis of fatty acid methyl esters into their corresponding fatty acids and alcohols—occur more rapidly than transesterification, thereby reducing canola oil conversion. Although the process efficiency at 100°C under similar conditions was lower than that at 85°C, a reaction temperature of 85°C was selected due to the safety and environmental issues. When the reaction temperature exceeds methanol's boiling point, a large amount of methanol vapor is produced, which is harmful to the environment. The conversion of 95.67% was achieved at a reflux temperature of 85°C.

To investigate the effect of catalyst amount on catalytic efficiency, a series of reactions were conducted using 0.1, 0.2, and 0.4 of 5La/ZSM-5 catalyst (corresponding to 5, 10, and 20 *wt* % catalysts to oil ratio, respectively) at 85°C for 7 h, with a fixed methanol-to-oil mass ratio of 5:1. The conversion percent of canola oil increased with increasing the catalyst dosage. The catalyst amount of 0.4 g (corresponding to 20 *wt* %) was therefore identified as the optimal catalyst dosage. As the amount of catalyst increases, the number of active sites for the reaction increases, facilitating the formation of methyl esters.

Based on the reaction stoichiometry, the theoretical molar ratio of alcohol to oil is 3:1. However, as reported in previous studies [47], higher molar ratios are typically employed to achieve higher conversion percents. According to Le Chatelier's principle, increasing the methanol concentration shifts the equilibrium of the transesterification reaction toward the forward direction, thereby accelerating the formation of methyl esters. On the other hand, increasing the alcohol content decreases the mixture's viscosity and enhances ester formation, as improved mixing increases mass transfer within the system. In

Table 7. Conversion percentages of canola oil in different conditions

No.	Catalyst	La (wt%)	Calcination temperature (°C)	Reaction temperature (°C)	Catalyst (wt%)	Methanol-to-oil mass ratio	Reaction time (h)	Conversion (%)
				La content				
1	0.5La/Z2S4	0.5	550	100	10	3:1	7	53.00
2	1La/Z2S4	1	550	100	10	3:1	7	71.00
3	2La/Z2S4	2	550	100	10	3:1	7	78.00
4	3La/Z2S4	3	550	100	10	3:1	7	84.30
5	4La/Z2S4	4	550	100	10	3:1	7	86.82
6	5La/Z2S4	5	550	100	10	3:1	7	95.42
7	6La/Z2S4	6	550	100	10	3:1	7	94.88
8	7La/Z2S4	7	550	100	10	3:1	7	85.29
				Calcination temperature				
9	5La/Z2S4	5	300	100	10	5:1	7	90.03
10	5La/Z2S4	5	400	100	10	5:1	7	98.05
11	5La/Z2S4	5	550	100	10	5:1	7	100
12	5La/Z2S4	5	700	100	10	5:1	7	85.29
				Transesterification reaction temperature				
13	5La/Z2S4	5	550	25	10	5:1	7	30.00
14	5La/Z2S4	5	550	40	10	5:1	7	53.08
15	5La/Z2S4	5	550	55	10	5:1	7	71.36
16	5La/Z2S4	5	550	70	10	5:1	7	84.30
17	5La/Z2S4	5	550	85	10	5:1	7	95.67
18	5La/Z2S4	5	550	100	10	5:1	7	100
19	5La/Z2S4	5	550	115	10	5:1	7	37.70
				Catalyst wt%				
20	5La/Z2S4	5	550	85	5	5:1	7	37.75
21	5La/Z2S4	5	550	85	10	5:1	7	95.00
22	5La/Z2S4	5	550	85	20	5:1	7	98.00
				Methanol-to-oil mass ratio				
23	5La/Z2S4	5	550	85	20	3:1	7	70.00
24	5La/Z2S4	5	550	85	20	5:1	7	84.00
25	5La/Z2S4	5	550	85	20	10:1	7	89.70
26	5La/Z2S4	5	550	85	20	15:1	7	100.00
27	5La/Z2S4	5	550	85	20	20:1	7	99.63
				Reaction time				
28	5La/Z2S4	5	550	85	20	15:1	1	60.00
29	5La/Z2S4	5	550	85	20	15:1	2	71.00
30	5La/Z2S4	5	550	85	20	15:1	3	84.48
31	5La/Z2S4	5	550	85	20	15:1	4	87.20
32	5La/Z2S4	5	550	85	20	15:1	5	89.32
33	5La/Z2S4	5	550	85	20	15:1	6	91.40
34	5La/Z2S4	5	550	85	20	15:1	7	100.00

this investigation, the methanol-to-oil ratio was optimized to maximize conversion efficiency.

The experiment conducted with an alcohol to-oil mass ratio of 15:1 achieved the highest conversion (100%) at 85°C and 20 *wt*% catalyst after 7 h (Entries 23-27 of Table 7). However, when the mass ratio exceeded 20:1, a slight decrease in oil conversion was observed, attributed to the competitive adsorption of methanol and oil molecules on the catalyst's active sites. The combination of excess methanol and its polar hydroxyl groups leads to the emulsification of glycerol and biodiesel formed during the reaction. This facilitates the reaction of glycerol with the esters, thus reducing the yield of the resulting biodiesel [53].

Finally, the effect of reaction time (including 1, 2, 3, 4, 5, 6, and 7 h) on the conversion% of canola oil was studied over 5La/Z2S4 catalyst at a temperature of 85°C, 20 *wt* % of catalyst, and a mass ratio of methanol-to-oil of 15:1(Entries 28-34 of Table 7). The conversion percentages of fatty acids increase with reaction time. Initially, the reaction rate was slow due to the mixing and dispersion of alcohol in the oil, but after a while it increased significantly. After approximately 7 h, the reaction achieved its highest conversion (100%). Beyond this point, further increases in reaction time did not affect the conversion.

Overall, the results indicate that the highest conversion percentage was obtained using the 5La/Z2S4 catalyst calcined at 550°C, under a reaction temperature of 85°C, with 20 *wt*% catalyst and a methanol-to-oil mass ratio of 15:1. It was also observed that 100% conversion can be achieved at a higher transesterification temperature of 100°C when using 10 *wt*% catalyst and a methanol-to-oil mass ratio of 5:1 under otherwise similar conditions. However, using 100°C to prepare biodiesel is not recommended due to excessive methanol evaporation and potential vapor leakage into the environment.

3. 9. Catalyst reusability

To assess the reusability of the 5La/Z2S4 catalyst, it was washed, dried, and subsequently reused in the transesterification reaction under the following conditions: 85°C, 3 h, 20 *wt*% catalyst, and a methanol-to-oil mass ratio of 15:1. The reaction efficiency was evaluated after reuse, which showed a significant decrease in conversion percentage (12.29%), which can be assigned to ester saturation at the active sites, reducing the number of active sites available for catalysis. Catalyst deactivation may also be due to changes in the catalyst structure during washing or drying processes.

3. 10. Investigation of the effect of transition metals on catalytic activity

In continuation, the synthesized zeolite was modified with various metals to enhance its catalytic performance. To investigate the catalytic activities of the prepared nano-catalysts, the transesterification of canola oil with methanol was conducted upon 5Ni/Z2S4, 5Cu/Z2S4, 5Co/Z2S4, 5Cr/Z2S4, and 0.8V-5La/Z2S4 catalysts for a reaction time of 3 h. The conversion percentage of canola oil is presented in Fig. 17, and the results show an explicit dependence of catalytic performance on the type of metal incorporated. The activity of the 5La/Z2S4 nano-catalyst was further increased by the addition of vanadium as a promoter, achieving a 100% conversion% after 3 h.

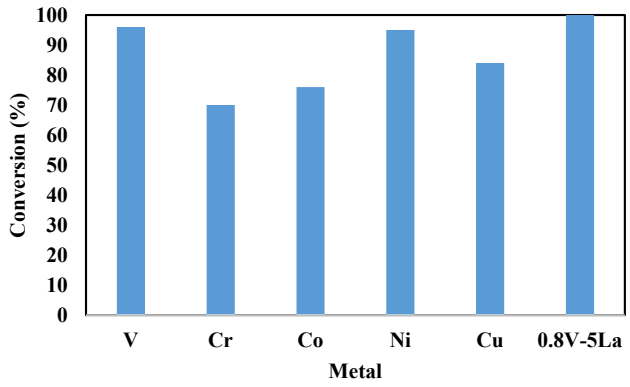

Fig. 17. Comparison of transition metals on the transesterification reaction of canola oil with methanol in calcination temperature of support=550°C, reaction temperature=85°C, mass ratio of methanol-to-oil 15:1, 5 wt % of catalyst, 3 h

Among the synthesized catalysts, those modified with nickel and vanadium exhibited the maximum catalytic efficiencies.

4. Conclusion

In the present study, HZSM-5 zeolite was synthesized using a seed-assisted and ultrasonic-assisted method. The obtained HZSM-5 was directly employed as seed for the preparation of efficient catalysts for biodiesel production, without the need for additional treatment. This synthesis method offers a cost-effective procedure for zeolite production. To design and develop a wide variety of catalysts to meet stringent quality, La impregnation on HZSM-5 has been considered. The catalytic activity of the prepared catalysts in the transesterification reaction was studied. Two distinct layers were formed during transesterification, in which the upper layer is biodiesel and the bottom layer is, essentially, glycerol. Therefore, the operating conditions for the transesterification of canola oil were optimized using the xLa/Z2S4 catalyst. The highest biodiesel production efficiency was achieved using the 5La/Z2S4 catalyst (calcination temperature is 550 ℃) containing 5 *wt*% lanthanum stabilized on zeolite under conditions of 85 ℃, 20 *wt*% of catalyst, methanol-to-oil mass ratio of 15:1, and a reaction time of 7 h.

Comparative experiments conducted with different catalysts revealed that the La supported Z2S4 catalyst shows the highest efficiency in biodiesel production. In order to compare the catalytic activity of 5La/Z2S4 with that of other catalysts stabilized with transition metals (V, Cr, Co, Cu, and Ni), the transesterification of canola oil with methanol was conducted under the optimum conditions previously determined using the 5La/Z2S4 catalyst. Furthermore, the transesterification reaction was performed in the absence of a catalyst, and the results showed that, in contrast to the catalytic reactions, the conversion percentage decreased significantly. The synthesized La/Z2S4 catalyst retained its catalytic activity after regeneration.

Acknowledgement

The authors thank the Alzahra Research Council for its financial support.

References

[1] J. Wang, W. Azam, Natural resource scarcity, fossil fuel energy consumption, and total greenhouse gas emissions in top emitting countries. Geoscience Frontiers. 15 (2024) 101757. https://doi.org/10.1016/j.gsf.2023.101757

[2] Y. M. Sani, W. M. A. W. Daud, A. R. Abdul Aziz, Activity of solid acid catalysts for bi-odiesel production: A critical review. Appl. Catal. A Gen. 470 (2014) 140–161. https://doi.org/10.1016/j.apcata.2013.10.052

[3] F. Perera, Pollution from Fossil-Fuel Combustion is the Leading Environmental Threat to Global Pediatric Health and Equity: Solutions Exist. Int. J. Environ. Res. Public Health. 15 (1) (2018) 16. https://doi.org/10.3390/ijerph15010016

[4] M. H. Pranta, H. M. Cho, A comprehensive review of the evolution of biodiesel production technologies. Energy Convers. Manag. 328 (2025) 119623. https://doi.org/10.1016/j.enconman.2025.119623

[5] S. Khan et al., Biodiesel Production from Algae to Overcome the Energy Crisis. HAYATI J. Biosci. 24 (2017) 163–167. https://doi.org/10.1016/j.hjb.2017.10.003

[6] J. H. Ng, H. K. Ng, S. Gan, Advances in Biodiesel Fuel for Application in Compression Ignition Engines. Clean Technol. Environ. Policy. 12 (2010) 459–493. https://doi.org/10.1007/s10098-009-0268-6

[7] O. M. Ali, R. Mamat, C. K. M. Faizal, Review of the effects of additives on biodiesel properties, performance, and emission features. J. Renew. Sustain. Energy. 5 (1) (2013) https://doi.org/10.1063/1.4792846

[8] M. Aydın, S. Uslu, M. Bahattin Çelik, Performance and emission prediction of a compression ignition engine fueled with biodiesel-diesel blends: A combined application of ANN and RSM based optimization. Fuel. 269 (2020) 117472. https://doi.org/10.1016/j.fuel.2020.117472

[9] B. Wahlund, J. Yan, M. Westermark, Increasing biomass utilisation in energy systems: A comparative study of CO2 reduction and cost for different bioenergy processing options. Biomass and Bioenergy. 26 (2004) 531–544. https://doi.org/10.1016/j.biombioe.2003.09.003

[10] S. J. Malode, K. K. Prabhu, R. J. Mascarenhas, N. P. Shetti, T. M. Aminabhavi, Recent advances and viability in biofuel production. Energy Convers. Manag. X. 10 (2020) 100070. https://doi.org/10.1016/j.ecmx.2020.100070

[11] S. X. Tan, S. Lim, H. C. Ong, Y. L. Pang, State of the art review on development of ultrasound-assisted catalytic transesterification process for biodiesel production. Fuel. 235 (2019) 886–907. https://doi.org/10.1016/j.fuel.2018.08.021

[12] M. Kadir Yesilyurt, C. Cesur, Biodiesel synthesis from Styrax officinalis L. seed oil as a novel and potential non-edible feedstock: A parametric optimization study through the Taguchi technique. Fuel. 265 (2020) 117025. https://doi.org/10.1016/j.fuel.2020.117025

[13] N. Mhetras, D. Gokhale, Sustainable biodiesel production: importance of feedstock re-sources and production methods. RSC Adv. 15 (2025) 26739-26754. https://doi.org/10.1039/D5RA03084F

[14] K. E. Low et al., Combinatorial Glycomic Analyses to Direct CAZyme Discovery for the Tailored Degradation of Canola Meal Non-Starch Dietary Polysaccharides. Microorganisms. 8 (2020) 1–27. https://doi.org/10.3390/

microorganisms8121888

[15] M. Santaraite, E. Sendzikiene, V. Makareviciene, K. Kazancev, Biodiesel Production by Lipase-Catalyzed in Situ Transesterification of Rapeseed Oil Containing a High Free Fatty Acid Content with Ethanol in Diesel Fuel Media. Energies. 13 (2020) https://doi.org/10.3390/en13102588

[16] D. M. DeMarini, E. Mutlu, S. H. Warren, C. King, M. I. Gilmour, W. P. Linak, Mutagenicity emission factors of canola oil and waste vegetable oil biodiesel: Comparison to soy biodiesel. Mutat. Res. - Genet. Toxicol. Environ. Mutagen. 846 (2019) 403057. https://doi.org/10.1016/j.mrgentox.2019.05.013

[17] M. A. Rajaeifar, B. Ghobadian, M. D. Heidari, E. Fayyazi, Energy Consumption and Greenhouse Gas Emissions of Biodiesel Production from Rapeseed in Iran. J. Renew. Sustain. Energy. 5 (6) (2013) 063134. https://doi.org/10.1063/1.4854596

[18] H. Kazemi, S. H. Bourkheili, B. Kamkar, A. Soltani, K. Gharanjic, N. M. Nazari, Estimation of greenhouse gas (GHG) emission and energy use efficiency (EUE) analysis in rainfed canola production (case study: Golestan province, Iran). Energy. 116 (2016) 694–700. https://doi.org/10.1016/j.energy.2016.10.010

[19] M. Ansari, H. Jamali, R. Ghanbari, M. H. Ehrampoush, P. Zamani, B. Hatami, Hetero-geneous solid acid catalysts for sustainable biodiesel production from wastewater-derived sludge: A systematic and critical review. Chem. Eng. J. Adv. 22 (2025) 100718-100731. https://doi.org/10.1016/j.ceja.2025.100718

[20] S. Chongkhong, C. Tongurai, P. Chetpattananondh, Renew. Continuous esterification for biodiesel production from palm fatty acid distillate using economical process. Energy. 34 (2009) 1059–1063. https://doi.org/10.1016/j.renene.2008.07.008

[21] A. P. S. Chouhan, A. K. Sarma, Modern heterogeneous catalysts for biodiesel produc-tion: A comprehensive review. Renew. Sustain. Energy Rev. 15 (2011) 4378–4399. https://doi.org/10.1016/j.rser.2011.07.112

[22] M. Agarwal, G. Chauhan, S. P. Chaurasia, K. Singh, Study of catalytic behavior of KOH as homogeneous and heterogeneous catalyst for biodiesel production. J. Taiwan Inst. Chem. Eng. 43 (2014) 89–94. https://doi.org/10.1016/j.jtice.2011.06.003

[23] B. Changmai, Ch. Vanlalveni, A. Prabhakar Ingle, R. Bhagat, S. Lalthazuala Rokhum, Widely used catalysts in biodiesel production: a review. RSC Adv. 10 (2020) 41625-41679. https://doi.org/10.1039/D0RA07931F

[24] C. Liu, P. Lv, Z. Yuan, F. Yan, W. Luo, The nanometer magnetic solid base catalyst for production of biodiesel. Renew. Energy. 35 (2010) 1531–1536. https://doi.org/10.1016/j.renene.2009.10.009

[25] S. Y. Chua et al., Biodiesel synthesis using natural solid catalyst derived from biomass waste — A review. J. Ind. Eng. Chem. 81 (2020) 41–60. https://doi.org/10.1016/j.jiec.2019.09.022

[26] A. O. Etim, P. Musonge, A. C. Eloka-Eboka, Effectiveness of biogenic waste-derived heterogeneous catalysts and feedstock hybridization techniques in biodiesel production. Biofuels, Bioprod. Biorefining. 14 (2020) 620–649. https://doi.org/10.1002/bbb.2094

[27] M. H. Nada, S. C. Larsen, Insight into seed-assisted template free synthesis of ZSM-5 zeolites. Microporous Mesoporous Mater. 239 (2017) 444–452. https://doi.org/10.1016/j.micromeso.2016.10.040

[28] D. P. Serrano, G. Centi, P. A. Diddams, J. Cejka, Outlooks for zeolite catalysts in a low-carbon scenario. Catalysis Today. 426 (2024) 114365. https://doi.org/10.1016/j.cattod.2023.114365

[29] E. F. Oliveira, L. D. Machado, R. H. Baughman, D. S. Galvao, Three-dimensional carbon nanotube networks from beta zeolite templates: Thermal stability and mechanical properties. Comput. Mater. Sci. 182 (2020) 109781. https://doi.org/10.1016/j.commatsci.2020.109781

[30] A. Palčić, V. Valtchev, Analysis and control of acid sites in zeolites. Appl. Catal. A Gen. 606 (2020) 117795. https://doi.org/10.1016/j.apcata.2020.117795

[31] W. Kim, J. C. Kim, S. Lee, J. Kim, R. Ryoo, Mesopore-selective incorporation of strong Brønsted acid catalytic sites via aluminium grafting on hierarchically porous siliceous MFI zeo-lite. Microporous Mesoporous Mater. 305 (2020) 110353. https://doi.org/10.1016/j.micromeso.2020.110353

[32] D. Vaičiukynienė, L. Jakevičius, A. Kantautas, V. Vaitkevičius, V. Vaičiukynas, K. Dvořák, Conversion of silica by-product into zeolites by thermo-sonochemical treatment. Ultrason. Sonochem. 72 (2021) 105426. https://doi.org/10.1016/j.ultsonch.2020.105426

[33] Q. Zhang, Sh. Gao, J. Yu, Metal Sites in Zeolites: Synthesis, Characterization, and Cataly-sis. Chem. Rev. 123 (2023) 6039-6106. https://doi.org/10.1021/acs.chemrev.2c00315

[34] D. Kerstens, B. Smeyers, J. Van Waeyenberg, Q. Zhang, J. Yu, B. F. Sels, State of the art and perspectives of hierarchical zeolites: practical overview of synthesis methods and use in catalysis. Adv. Mater. 32 (2020) 1–47. https://doi.org/10.1002/adma.202004690

[35] M. Haghighi, S. Bakhshi, and S. Gooneh-farahani, Enhanced catalytic cracking of tetra-decane over nano-structure porous ZSM-5 and ZSM-11 catalysts. Mater. Sci. Eng. B. 263 (2021) 114894. https://doi.org/10.1016/j.mseb.2020.114894

[36] Song et al., Synthesis and Characterization of Hierarchical ZSM-5 Zeolites with Outstanding Mesoporosity and Excellent Catalytic Properties. Nanoscale Res Lett. 13 (2018) 364. https://doi.org/10.1186/s11671-018-2779-8

[37] K. P. Dey, S. Ghosh, M. K. Naskar, Organic template-free synthesis of ZSM-5 zeolite particles using rice husk ash as silica source. Ceram. Int. 39 (2013) 2153–2157. https://doi.org/10.1016/j.ceramint.2012.07.083

[38] J. C. Jansen, F. J. van der Gaag, H. van Bekkum, Identification of ZSM-type and other 5-ring containing zeolites by i.r. spectroscopy. Zeolites. 4 (1984) 369–372. https://doi.org/10.1016/0144-2449(84)90013-7

[39] S. S. Vieira, Z. M. Magriotis, N. A. V. Santos, A. A. Saczk, C. E. Hori, P. A. Arroyo, Biodiesel production by free fatty acid esterification using lanthanum (La3+) and HZSM-5 based catalysts. Bioresour. Technol. 133 (2013) 248–255. https://doi.org/10.1016/j.biortech.2013.01.107

[40] S. S. Vieira et al., Production of biodiesel using HZSM-5

zeolites modified with citric acid and SO42−/La2O3. Catal. Today. 279 (2017) 267–273. https://doi.org/10.1016/j.cattod.2016.04.014

[41] Y. Li, H. Liu, J. Zhu, P. He, P. Wang, H. Tian, DFT study on the accommodation and role of La species in ZSM-5 zeolite. Microporous Mesoporous Mater. 142 (2011) 621–628. https://doi.org/10.1016/j.micromeso.2011.01.007

[42] C. W. Lee, W. J. Lee, Y. K. Park, S. E. Park, Catalytic hydroxylation of benzene over vanadium containing nolecular sieves. Catal. Today. 61 (2000) 137–141. https://doi.org/10.1016/S0920-5861(00)00357-6

[43] W. Song, R. E. Justice, C. A. Jones, V. H. Grassian, S. C. Larsen, Synthesis, Characteriza-tion, and Adsorption Properties of Nanocrystalline ZSM-5. Langmuir. 20 (2004) 8301–8306. https://doi.org/10.1021/la049516c

[44] A. Philippou, M. W. Anderson, Aldol-Type Reactions over Basic Microporous Titano-silicate ETS-10 Type Catalysts. J. Catal. 189 (2000) 395–400. https://doi.org/10.1006/jcat.1999.2705

[45] Z. Li et al., Synthesis and evaluation of mesopore structured ZSM-5 and a CuZSM-5 catalyst for NH3-SCR reaction: studies of simulated exhaust and engine bench testing. RSC Adv. 6 (2016) 102570–102581. https://doi.org/10.1039/c6ra20237c

[46] S. Yan, S. O. Salley, K. Y. Simon Ng, Simultaneous transesterification and esterification of unrefined or waste oils over ZnO-La2O3 catalysts. Appl. Catal. A Gen. 353 (2009) 203–212. https://doi.org/10.1016/j.apcata.2008.10.053

[47] L. C. Meher, D. Vidya Sagar, S. N. Naik, Technical aspects of biodiesel production by transesterification—a review. Renew. Sustain. Energy Rev. 10 (2006) 248–268. https://doi.org/10.1016/j.rser.2004.09.002

[48] A. Demirbas, Biodiesel production from vegetable oils via catalytic and non-catalytic supercritical methanol transesterification methods. Prog. Energy Combust. Sci. 31 (2005) 466–487. https://doi.org/10.1016/j.pecs.2005.09.001

[49] L. Lin et al., Evidence of health benefits of canola oil. Nutr. Rev., 71 (2013) 370–385. https://doi.org/10.1111/nure.12033

[50] S. Rezania, S. Mahdinia, B. Oryani, J. Cho, E. E. Kwon, A. Bozorgian, H. Rashidi Nodeh, N. Darajeh, K. Mehranzamir, Biodiesel production from wild mustard (Sinapis Arvensis) seed oil using a novel heterogeneous catalyst of LaTiO3 nanoparticles. Fuel. 307 (2022) 121759. https://doi.org/10.1016/j.fuel.2021.121759

[51] H. Maleki, M. Kazemeini, A. S. Larimi, F. Khorasheh, Transesterification of canola oil and methanol by lithium impregnated CaO–La2O3 mixed oxide for biodiesel synthesis. J. Ind. Eng. Chem. 47 (2017) 399–404. https://doi.org/10.1016/j.jinech.2017.01.037

[52] Z. Helwani, M. R. Othman, N. Aziz, W. J. N. Fernando, J. Kim, Technologies for pro-duction of biodiesel focusing on green catalytic techniques: A review. Fuel Process. Technol. 90 (2009) 1502–1514. https://doi.org/10.1016/j.fuproc.2009.07.016

[53] L. R. Kumar, S. K. Yellapu, R. D. Tyagi, X. Zhang, A review on variation in crude glycer-ol composition, bio-valorization of crude and purified glycerol as carbon source for lipid pro-duction. Bioresour. Technol. 293 (2019) 122155